Neuropsychologia xxx (xxxx) xxx–xxx

Contents lists available at ScienceDirect

Neuropsychologia

journal homepage: www.elsevier.com/locate/neuropsychologia

# Modality-independent encoding of individual concepts in the left parietal cortex

Giacomo Handjaras[a,c], Andrea Leo[a,c,*], Luca Cecchetti[a,c], Paolo Papale[a,c], Alessandro Lenci[b], Giovanna Marotta[b], Pietro Pietrini[c], Emiliano Ricciardi[c]

[a] Laboratory of Clinical Biochemistry and Molecular Biology, University of Pisa, Pisa, Italy
[b] Department of Philology, Literature, and Linguistics, University of Pisa, Pisa 56126, Italy
[c] Molecular Mind Lab, IMT School for Advanced Studies Lucca, Lucca 55100, Italy

ARTICLE INFO

*Keywords:*
Semantic representation
Blindness
Representational similarity encoding analysis
FMRI
GIST
Shock-graph

ABSTRACT

The organization of semantic information in the brain has been mainly explored through category-based models, on the assumption that categories broadly reflect the organization of conceptual knowledge. However, the analysis of concepts as individual entities, rather than as items belonging to distinct superordinate categories, may represent a significant advancement in the comprehension of how conceptual knowledge is encoded in the human brain.

Here, we studied the individual representation of thirty concrete nouns from six different categories, across different sensory modalities (i.e., auditory and visual) and groups (i.e., sighted and congenitally blind individuals) in a core hub of the semantic network, the left angular gyrus, and in its neighboring regions within the lateral parietal cortex. Four models based on either perceptual or semantic features at different levels of complexity (i.e., low- or high-level) were used to predict fMRI brain activity using representational similarity encoding analysis. When controlling for the superordinate component, high-level models based on semantic and shape information led to significant encoding accuracies in the intraparietal sulcus only. This region is involved in feature binding and combination of concepts across multiple sensory modalities, suggesting its role in high-level representation of conceptual knowledge. Moreover, when the information regarding superordinate categories is retained, a large extent of parietal cortex is engaged. This result indicates the need to control for the coarse-level categorial organization when performing studies on higher-level processes related to the retrieval of semantic information.

## 1. Introduction

The organization of semantic information in the human brain has been primarily explored through models based on categories. This *domain-specific* approach relies on the assumption, supported by neuropsychological and neuroimaging observations, that the categories of language (e.g., *faces, places, body parts, tools, animals*) broadly reflect the organization of conceptual knowledge in the human brain (Kemmerer, 2016; Mahon and Caramazza, 2009).

However, rather than being limited to differentiate among a small number of broad superordinate categories, a deeper comprehension of conceptual knowledge organization at a neural level should characterize the semantic representation of individual entities (Charest et al., 2014; Clarke and Tyler, 2015; Mahon and Caramazza, 2011). In fact, despite the strong evidence in favor of a categorial organization of conceptual knowledge in the brain (Gainotti, 2010; Pulvermuller, 2013), category-based models are over-simplified and often do not take into account those perceptual and semantic features (e.g., shape, size, function, emotion) involved in the finer-grained discrimination of individual concepts (Clarke and Tyler, 2015; Kemmerer, 2016). Typically, semantic studies limit at controlling those variables within broader and heterogeneous categories, thus restricting the emerging of individual item processing (Baldassi et al., 2013; Bona et al., 2015; Bracci and Op de Beeck, 2016; Ghio et al., 2016; Kaiser et al., 2016; Proklova et al., 2016; Vigliocco et al., 2014; Wang et al., 2016). Furthermore, broader categories are often affected by a high degree of collinearity, as stimuli belonging to highly dissimilar categories according to a sensory-based description (e.g., *faces* and *places*), may also be very dissimilar according to their semantic characterization. Thus, the labeling of certain brain regions might rely either on perceptual or semantic features (Carlson et al., 2014; Fernandino et al., 2016; Jozwik et al., 2016; Khaligh-Razavi and Kriegeskorte, 2014).

* Correspondence to: Molecular Mind Lab, IMT School for Advanced Studies Lucca, Piazza San Francesco 19, Lucca 55100, Italy.
*E-mail address:* and.leov@gmail.com (A. Leo).

http://dx.doi.org/10.1016/j.neuropsychologia.2017.05.001
Received 1 November 2016; Received in revised form 29 April 2017; Accepted 2 May 2017

In addition, the transition from lower-level sensory-based representations towards higher-level conceptual representations is still ill defined. For instance, how entities that are similar for one or more perceptual features (e.g., shape: a *tomato* and a *ball*) are represented in the brain as semantically different remains to be understood (Bi et al., 2016; Clarke and Tyler, 2015; Kubilius et al., 2014; Rice et al., 2014; Tyler et al., 2013; Wang et al., 2016, 2015; Watson et al., 2016).

To assess the extent to which the category-based organization relies on sensory information, our group recently adopted a property generation paradigm in sighted and congenitally blind individuals to demonstrate that the representation of semantic categories relies on a modality-independent brain network (Handjaras et al., 2016). Furthermore, the analysis of individual cortical regions showed that only a few of them (i.e., inferior parietal lobule and parahippocampal gyrus) contained distinct representations of items belonging to different semantic categories across presentation modalities (i.e., pictorial, verbal visual and verbal auditory forms or verbal auditory form in congenitally blind individuals) (Handjaras et al., 2016).

In the present study, we intended to describe the representation, across different presentation modalities, of each of the thirty concrete nouns from six different categories, using part of the same dataset of Handjaras and colleagues (2016). Instead of encoding semantic information using a category-based model, here we characterized the representation of the individual entities using a recent method for fMRI data analysis, called representational similarity encoding (Anderson et al., 2016b), to combine representational similarity analysis and model-based encoding. Moreover, the conceptual representation was evaluated by focusing on the entities within each category (e.g., fruits: *apple* vs. *cherry*). This *within-category* encoding is therefore resistant to the effect of category membership and represents an adequate perspective to study how single concepts are processed in the brain. To disentangle the role of perceptual or semantic features and of their complexity (i.e., low- or high-level), we aimed at predicting brain activity using similarity encoding with four models: two semantic models that considered either the complete set of language-based features or a subset of these features related to perceptual properties only (Lenci et al., 2013), and two perceptual models, which provided higher-level descriptions of object shape, or merely focused on low-level visual features (Oliva and Torralba, 2001; van Eede et al., 2006).

We focused the single-item encoding analysis on the angular gyrus and its neighboring regions within the left parietal cortex. The angular region has been solidly associated to a wide gamut of semantic tasks, and its activity during retrieval and processing of concrete nouns or combination of concepts (Binder et al., 2009; Price et al., 2015; Seghier, 2013) makes this region a strong candidate for semantic processing at a finer, single-item level. More importantly, neighboring regions to the angular gyrus within the left lateral parietal cortex have been involved, to a different extent, in semantic processing, thus indicating the need for a more comprehensive characterization of conceptual representations within the parietal lobe (Binder et al., 2009; Jackson et al., 2016; Price, 2012). Therefore, the analyses were performed in a larger map of the left lateral parietal cortex that centered on the angular gyrus, as defined on both anatomical and functional criteria. The definition of different Regions of Interest (ROIs) assessed the different degree of involvement of specific regions in processing of individual concepts, and how such a processing is influenced by sensory modality.

## 2. Materials and methods

A representational similarity encoding (Anderson et al., 2016b) was applied to data collected in a fMRI experiment, in which sighted and blind participants were instructed to mentally generate properties related to a set of concrete nouns, as described in details in our previous study (Handjaras et al., 2016). In brief, participants were divided in four groups according to the stimulus presentation modality (i.e., pictorial, verbal visual and verbal auditory forms for sighted individuals and verbal auditory form for congenitally blind individuals). Two semantic models were built on the set of concrete nouns and two alternative perceptual models were derived from the pictorial form of the stimuli. Of both semantic and perceptual models, one was a descriptor of high-level features and one relied on lower-level information. The four models were then used to encode the specific brain activity pattern of each concept, in each group of subjects.

### 2.1. Brief summary of the Handjaras et al. (2016) fMRI protocol and preprocessing

Brain activity was measured in fMRI with a slow event-related paradigm (gradient echo echoplanar images GRE-EPI, GE SIGNA at 3 T, equipped with an 8-channel head coil, TR 2.5 s, FA: 90°, TE 40 ms, FOV = 24 cm, 37 axial slices, voxel size $2 \times 2 \times 4$ mm) in 20 right-handed volunteers during a property generation task after either visual or auditory presentation of thirty concrete nouns of six semantic categories (i.e., vegetables, fruits, mammals, birds, tools, vehicles) (please refer to Supplementary materials for the list of nouns). Two semantic categories (e.g., natural and artificial places) from Handjaras et al. (2016) were excluded here due to a specific limitation of the shape-based perceptual model which required segmented stimuli (e.g., objects). Participants were divided into four groups accordingly to the stimulus presentation format: five sighted individuals were presented with a pictorial form of the forty nouns (M/F: 2/3 mean age ± SD: 29.2 ± 12.8 yrs), five sighted individuals with a verbal visual form (i.e., written Italian words) (M/F: 3/2 mean age ± SD: 36.8 ± 11.9 yrs), five sighted individuals with a verbal auditory form (i.e., spoken Italian words) (M/F: 2/3 mean age ± SD: 37.2 ± 15 yrs) and five congenitally blind with a verbal auditory form (M/F: 2/3 mean age ± SD: 36.4 ± 11.7 yrs). High resolution T1-weighted spoiled gradient recall images were obtained to provide detailed brain anatomy.

During the visual presentation modality, subjects were presented either with images representing the written word (verbal visual form) or color pictures of concrete objects (pictorial form). Stimulus presentation lasted 3 s and was followed by a 7 s-inter stimulus interval (ISI). During the auditory presentation modality, subjects were asked to listen to about 1 s-long words – referring to the same concrete nouns above – followed by 9 s ISI. During each 10 s-long trial, participants were instructed to mentally generate a set of features related to each concrete noun. Each run had two 15 s-long blocks of rest, at its beginning and end, to obtain a measure of baseline activity. The stimuli were presented four times, using, for each repetition, a different image (for pictorial stimuli) or speaker (for auditory stimuli). The presentation order was randomized across repetitions and the stimuli were organized in five runs.

The AFNI software package (Cox, 1996) was used to preprocess functional imaging data. All volumes from the different runs were temporally aligned, corrected for head movement, spatially smoothed (4 mm) and normalized. Subsequently, a multiple regression analysis was performed to obtain *t*-score response patterns of each stimulus, which were included in the subsequent analyses. Each stimulus was modeled using five tent functions which covered the entire interval from its onset up to 10 s, with a time step of 2.5 s. Only the *t*-score response patterns of the fourth tent function (7.5 s after stimulus onset), averaged across the four repetitions, were used as estimates of the BOLD response for each stimulus (Handjaras et al., 2015; Leo et al., 2016). Afterwards, FMRIB's Nonlinear Image Registration tool (FNIRT) was used to register the fMRI volumes to standard space (MNI-152) and to resample the acquisition matrix to a 2 mm iso-voxel (Andersson et al., 2007; Smith et al., 2004).

### 2.2. Regions of interest

For our measurement of single-item semantic information, we first defined a mask of the left angular gyrus both using the Automated

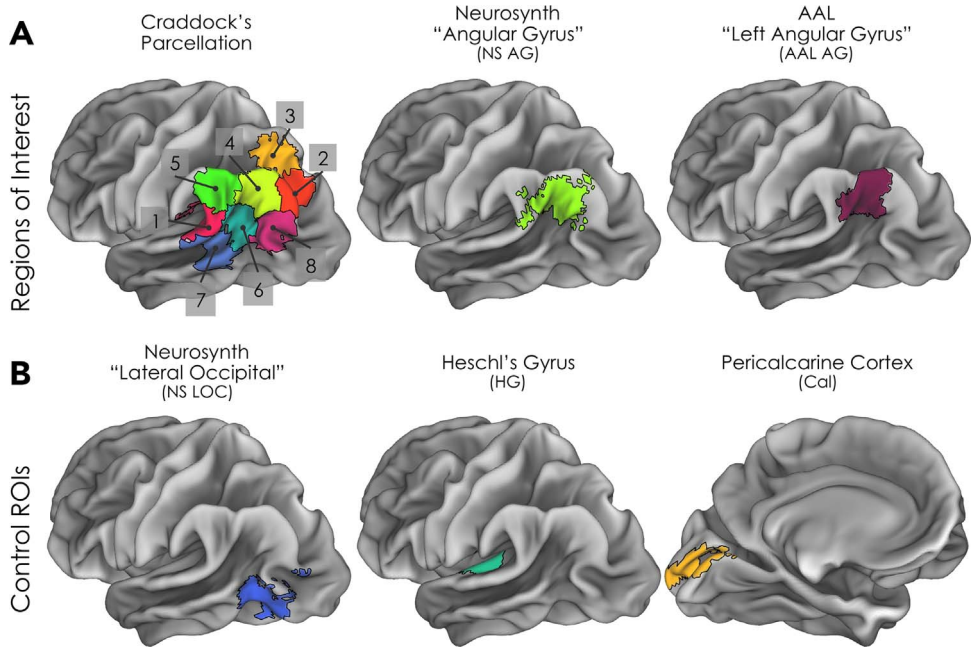


**Fig. 1. ROIs**. As regions of interest, the left lateral parietal cortex was parcellated using the brain atlas by Craddock et al. (2012), while the functional and the anatomical masks of the angular gyrus were extracted from the Neurosynth database (Yarkoni et al., 2011) and the Automated Anatomical Labeling (AAL) Atlas respectively (Tzourio-Mazoyer et al., 2002) (Panel A). As control regions, we defined the left lateral occipital complex (LOC) using the Neurosynth database, and the bilateral Heschl gyri (HG) and the bilateral calcarine and pericalcarine cortex (Cal) using the Jülich histological atlas (Eickhoff et al., 2007) (Panel B).

Anatomical Labeling (AAL) Atlas (Tzourio-Mazoyer et al., 2002) and from a functional meta-analysis using the Neurosynth database (Yarkoni et al., 2011).

Due to the fact that recent evidence shows that semantic processing, albeit mostly centered on the angular gyrus, does involve neighboring regions as well (Binder et al., 2009; Jackson et al., 2016; Price, 2012), we expanded the area of interest to include a larger extent of left parietal cortex, using a mask divided into subregions which could be analyzed separately. First, the functional mask extracted from the Neurosynth database was superimposed to the functional brain atlas by Craddock et al. (2012). A parcellation to 200 ROIs was chosen using the temporal correlation between voxels time-courses as similarity metric; this criterion ensures high anatomic homology and interpretability (Craddock et al., 2012). At last, eight ROIs were defined in the left lateral parietal cortex, which overlapped, at least partially, with the left angular gyrus defined via Neurosynth meta-analysis (Figs. 1, 3 and Table 1).

The bilateral Heschl gyri (HG) and the bilateral calcarine and pericalcarine cortex (Cal) were selected as control regions to assess whether the different presentation modalities could affect primary sensory regions. The HG and Cal regions were defined using the Jülich histological atlas of the FMRIB Software Library (Eickhoff et al., 2007; Smith et al., 2004). In addition, to control for the role of high-level perceptual features, we used the Neurosynth database and the mask obtained from its meta-analytic map to define the left lateral occipital complex (LOC), a region involved in shape processing (Malach et al., 1995). The organization and spatial location of the regions of interest are represented in Table 1 and Fig. 1.

### 2.3. Semantic models

The Blind Italian Norming Data (BLIND) set, validated in an independent Italian sample of blind and sighted participants, was used to define the semantic model for the similarity encoding (Lenci et al., 2013). The concrete nouns of the BLIND study were a set of normalized stimuli that belong to various biological and artificial semantic categories, most of which are shared with previous norming studies (Connolly et al., 2007; Kremer and Baroni, 2011; McRae et al., 2005). In the BLIND study, sighted and congenitally blind participants were presented with concept names and were asked to verbally list the features that describe the entities the words refer to. The features produced by the subjects were not limited to sensory attributes of the stimuli (e.g., shape, size, color) but also included high-level properties, such as associated events and abstract features (Lenci et al., 2013). The collected features were extracted, pooled across subjects to derive averaged representations of the nouns, using subjects' production frequency as an estimate of feature salience (Handjaras et al., 2016; Lenci et al., 2013; Mitchell et al., 2008). This procedure provided a feature space of 812 dimensions (properties) for sighted and 743 for blind participants. As depicted in Fig. 2, the collected features were used to assemble two semantic models for both sighted and blind individuals: one based on the whole feature space (i.e., high-level semantic model), one restricted to the perceptual features only (i.e., Property of Perceptual Type, PPE), corresponding to those qualities that can be directly perceived, such as magnitude, shape, taste, texture, smell, sound and color (i.e., low-level semantic model) (Wu and Barsalou, 2009; Lenci et al., 2013).

Subsequently, representational spaces (RSs) were derived from the semantic models using correlation dissimilarity index (one minus Pearson's r), obtaining four group-level dissimilarity matrices (i.e., for sighted and blind subjects) (Fig. 2).

### 2.4. Perceptual models

A high-level perceptual model was obtained from the shape features of the thirty images. First, all the pictorial stimuli were manually segmented and binarized. A skeletal representation of each stimulus was then computed by performing the medial axis transform (Blum, 1973). The dissimilarity between each pair of skeletal representations was then computed using the ShapeMatcher algorithm (http://www.cs.toronto.edu/~dmac/ShapeMatcher/index.html; van Eede et al., 2006) which builds the shock-graphs of each object and then estimates their pairwise distance by computing the deformation needed in order to match their shapes (Sebastian et al., 2004). The distances were then

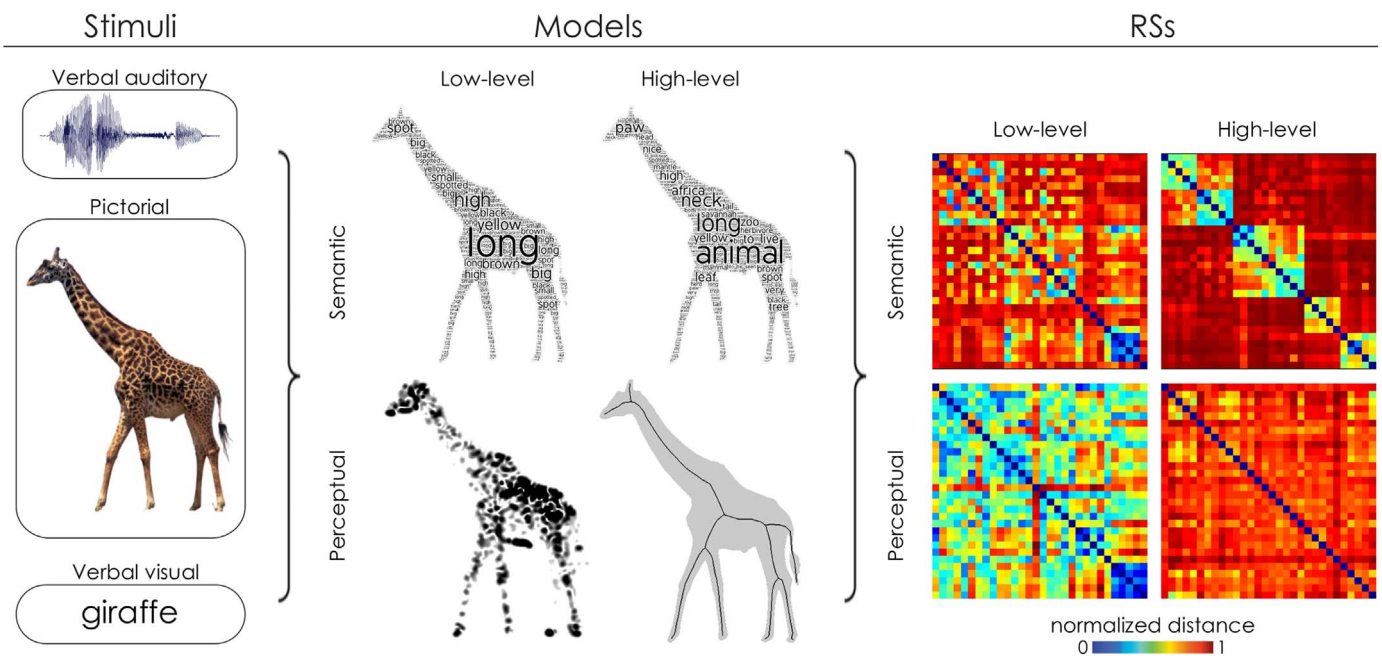


**Fig. 2. Models.** Figure depicts, on the left, the different presentation modalities used to evoke conceptual representations (pictorial, verbal visual and verbal auditory forms for sighted individuals and verbal auditory form for congenitally blind individuals). In the middle, the four models used for the encoding analyses are defined. Two semantic models, illustratively represented using word clouds, were built on the features generated in a behavioral experiment based on a property-generation task (Lenci et al., 2013): the high-level model was based on the whole set of linguistic features while the low-level one was defined on a subset of these features restricted to perceptual properties. Moreover, two perceptual models were obtained from the pictorial form of the stimuli: the high-level perceptual model was built on the shape features of the images through shock-graphs (Sebastian et al., 2004), while the low-level one was the GIST based on Gabor filters (Oliva and Torralba, 2001). For example, according to the high-level semantic model a *screwdriver* was very similar to a *hammer*, while according to the high-level shape-based perceptual model, a *screwdriver* was more similar to a *pencil* than to a *hammer*. The Representational Spaces (RSs) extracted from the four models are depicted on the right. Dissimilarity measures are reported in details in the Methods section.

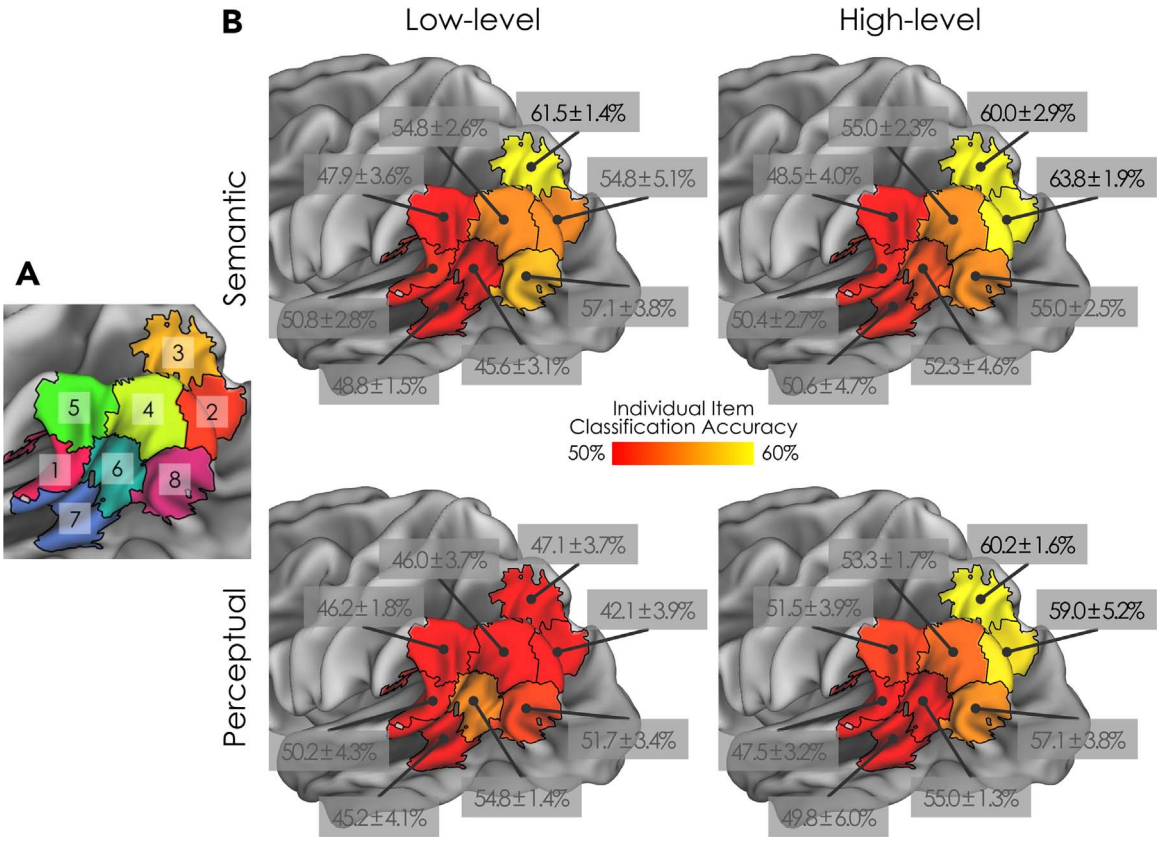


**Fig. 3. Encoding results.** Figure depicts the mean accuracy across presentation modalities of the representational similarity encoding analysis of the four models in the left lateral parietal cortex. The significant accuracy values ($p < 0.05$, Bonferroni corrected) are reported in bold font, the other values were not significant. Detailed results are reported for each ROI in Tables 3–6.

**Table 1**
ROIs. Here are reported Volume (in μL), X, Y and Z coordinates in MNI space (in mm) for the center of mass of each region. L Ang AAL and L Ang NS refer to the functional mask of the angular gyrus extracted from the Neurosynth database (Yarkoni et al., 2011) and the anatomical definition of the angular gyrus using the Automated Anatomical Labeling (AAL) Atlas (Tzourio-Mazoyer et al., 2002) respectively. ID ROI indicates the number of each region of Fig. 3 with the corresponding identification number (ID Craddock) from the atlas by Craddock et al. (2012).

| ID ROI | ID Craddock | Volume | X | Y | Z |
|---|---|---|---|---|---|
| 1 | 6 | 5824 | −56 | −43 | 23 |
| 2 | 22 | 6912 | −27 | −78 | 33 |
| 3 | 27 | 5888 | −24 | −68 | 50 |
| 4 | 49 | 6336 | −43 | −68 | 38 |
| 5 | 99 | 5632 | −52 | −50 | 41 |
| 6 | 110 | 6912 | −49 | −60 | 20 |
| 7 | 130 | 7424 | −57 | −49 | 6 |
| 8 | 188 | 6208 | −43 | −76 | 17 |
| Ang AAL | # | 9176 | −45 | −61 | 36 |
| Ang NS | # | 11424 | −47 | −64 | 33 |

averaged across the four repetitions of each pictorial stimulus, which corresponded to four different pictures, to produce a shape-based RS. This high-level perceptual description was used as a model to predict brain activity, similarly to what performed on fMRI data by other authors (Leeds et al., 2013).

Furthermore, to assess whether the patterns of neural response could be predicted also by differences in low-level image statistics of the different pictorial stimuli, we built a RS based on visual features (Oliva and Torralba, 2001; Rice et al., 2014). A global description of the spatial frequencies of each color image seen by the subjects during the pictorial presentation modality was estimated using the GIST model (Oliva and Torralba, 2001). Briefly, a GIST descriptor was computed by sampling the responses to Gabor filters with four different sizes and eight orientations; the GIST descriptor of each item was obtained by averaging the GIST descriptors of the four stimuli representing the item. The GIST descriptor of each item were then normalized and compared to each other using correlation dissimilarity index, generating a RS which was used as a low-level, perceptual model.

For each RS of the four models, the *within-category* information was extracted, normalized within each category scaling to the maximum distance and compared across models ($p < 0.05$, two tailed test, Bonferroni corrected for the number of comparisons, i.e., 15) (Table 2). Subsequently, *within-category* information of each model was used for the similarity encoding.

### 2.5. Representational similarity encoding analysis

The similarity encoding was recently proposed to merge representational similarity analysis and model-based encoding (Anderson et al., 2016b). In this approach, two RSs, one derived from neural and one from semantic or perceptual data, are compared each other using a leave-two-stimulus-out strategy: the two left out vectors from both matrices are matched using the correlation coefficient hence to generate an accuracy measure. This approach is resistant to overfitting issues and does not require parameters estimation (for further details, please refer to Anderson et al., 2016b).

The RSs from fMRI data were computed within each ROI and subject, using the correlation distance. For each presentation modality, the five single-subject RSs were averaged and the resulting group-level RSs were compared to the models RS as specified above. The analysis was limited to the five concrete nouns within each of the six categories, thus performing only 60 comparisons (i.e., *within-category* individual item encoding) instead of all the 435 comparisons (i.e., *among-categories* individual item encoding).

The standard error of the accuracy value was estimated using a bootstrapping procedure (1000 iterations) (Efron and Tibshirani, 1994). Finally, to assess the significance of the encoding analysis, the resulting accuracy value was tested against the null distribution with a permutation test in which both the neural and behavioral matrices were shuffled (1000 permutations, one-tailed rank test).

Moreover, within each ROI, accuracies of each presentation modality were averaged. The significance level was calculated by averaging null distributions obtained with a fixed permutation schema across presentation modalities (Nichols and Holmes, 2002). The averaged accuracy was subsequently tested with a one-tailed rank test (1000 permutations).

Accuracies across presentation modalities were reported in Tables 3–6, while the averaged accuracy across presentation modalities was represented onto a brain mesh in Fig. 3. All the p-values of the accuracies in Tables 3–6 were reported as uncorrected for multiple comparisons. Results from the left parietal cortex were corrected for Bonferroni when applicable (by adjusting the raw p-values evaluating the eight ROIs from the Craddock's Atlas).

The model definition and the similarity encoding approaches were accomplished by using Matlab (Matworks Inc., Natick, MA, USA), while Connectome Workbench was used to render the brain meshes in Figs. 1, 3, and 4B.

In addition, an alternative procedure based on the discrimination of each individual concrete noun irrespective of their membership to one of the six semantic categories (i.e., *among-categories* individual item encoding) was performed using the high-level semantic model only: this procedure aimed at measuring the impact of the categorial organization on the classification accuracy (see Supplementary materials).

## 3. Results

The combined procedure to identify the angular gyrus on an

**Table 2**
**Models' collinearities.** Table reports the Pearson's r correlation coefficient between each model.

| | high-level semantic model in sighted | high-level semantic model in blind | low-level semantic model in sighted | low-level semantic model in blind | high-level perceptual model | low-level perceptual model |
|---|---|---|---|---|---|---|
| **high-level semantic model in sighted** | | r = 0.68, p < 0.0001* | r = 0.23, p = 0.0714 | r = 0.16, p = 0.2231 | r = 0.28, p = 0.0301 | r = −0.14, p = 0.3005 |
| **high-level semantic model in blind** | | | r = 0.05, p = 0.7253 | r = 0.37, p = 0.0037 | r = 0.19, p = 0.1391 | r = −0.01, p = 0.9214 |
| **low-level semantic model in sighted** | | | | r = 0.33, p = 0.0095 | r = 0.10, p = 0.4430 | r = −0.06, p = 0.6521 |
| **low-level semantic model in blind** | | | | | r = 0.19, p = 0.1459 | r = 0.23, p = 0.0740 |
| **high-level perceptual model** | | | | | | r = −0.07, p = 0.6126 |
| **low-level perceptual model** | | | | | | |

* Indicates a significant correlation ($p < 0.05$, Bonferroni corrected).

**Table 3**
***Within-category* individual item encoding accuracies for the high-level semantic model**. Here are reported the accuracies in each ROI of the encoding procedure in each presentation modality (mean ± standard error) for the semantic model based on the whole linguistic feature space. For Ang AAL, Ang NS, LOC, HG and Cal, please refer to Fig. 1.

| ID ROI | Sighted Pictorial | Sighted Verbal Visual | Sighted Verbal Auditory | Blind Verbal Auditory | Average across modalities |
|---|---|---|---|---|---|
| 1 | 57.5 ± 4.2%, p = 0.150 | 51.7 ± 5.3%, p = 0.384 | 45.0 ± 3.8%, p = 0.746 | 47.5 ± 4.4%, p = 0.602 | 50.4 ± 2.7%, p = 0.459 |
| 2 | 62.5 ± 3.8%, p = 0.034 | 60.0 ± 4.4%, p = 0.059 | 69.2 ± 3.6%, p < 0.001* | 63.3 ± 3.1%, p = 0.034 | 63.8 ± 1.9%, p < 0.001* |
| 3 | 67.5 ± 4.2%, p = 0.008 | 56.7 ± 4.1%, p = 0.168 | 54.2 ± 4.4%, p = 0.254 | 61.7 ± 4.1%, p = 0.049 | 60.0 ± 2.9%, p = 0.005* |
| 4 | 53.3 ± 4.7%, p = 0.297 | 55.8 ± 4.7%, p = 0.184 | 60.8 ± 4.2%, p = 0.062 | 50.0 ± 4.8%, p = 0.491 | 55.0 ± 2.3%, p = 0.089 |
| 5 | 59.2 ± 4.8%, p = 0.107 | 40.8 ± 3.8%, p = 0.873 | 50.0 ± 4.6%, p = 0.468 | 44.2 ± 3.5%, p = 0.756 | 48.5 ± 4.0%, p = 0.651 |
| 6 | 64.2 ± 4.2%, p = 0.024 | 50.8 ± 3.7%, p = 0.402 | 41.7 ± 4.4%, p = 0.863 | 52.5 ± 4.7%, p = 0.347 | 52.3 ± 4.6%, p = 0.240 |
| 7 | 56.7 ± 5.0%, p = 0.159 | 60.0 ± 4.0%, p = 0.074 | 40.0 ± 3.7%, p = 0.910 | 45.8 ± 5.3%, p = 0.683 | 50.6 ± 4.7%, p = 0.415 |
| 8 | 54.2 ± 4.1%, p = 0.283 | 58.3 ± 3.9%, p = 0.098 | 48.3 ± 4.1%, p = 0.575 | 59.2 ± 4.2%, p = 0.090 | 55.0 ± 2.5%, p = 0.073 |
| Ang AAL | 49.2 ± 4.9%, p = 0.530 | 46.7 ± 4.4%, p = 0.640 | 61.7 ± 4.1%, p = 0.052 | 57.5 ± 4.5%, p = 0.146 | 53.8 ± 3.5%, p = 0.137 |
| Ang NS | 58.3 ± 4.4%, p = 0.114 | 51.7 ± 5.5%, p = 0.373 | 55.0 ± 4.1%, p = 0.227 | 53.3 ± 4.2%, p = 0.308 | 54.6 ± 1.4%, p = 0.108 |
| HG | 47.5 ± 3.3%, p = 0.605 | 56.7 ± 4.8%, p = 0.172 | 51.7 ± 4.4%, p = 0.372 | 50.8 ± 4.5%, p = 0.444 | 51.7 ± 1.9%, p = 0.316 |
| Cal | 45.0 ± 3.8%, p = 0.734 | 56.7 ± 4.4%, p = 0.179 | 59.2 ± 4.5%, p = 0.075 | 56.7 ± 4.1%, p = 0.170 | 54.4 ± 3.2%, p = 0.120 |
| LOC | 58.3 ± 3.7%, p = 0.121 | 59.2 ± 3.8%, p = 0.087 | 40.0 ± 3.2%, p = 0.902 | 49.2 ± 4.3%, p = 0.509 | 51.7 ± 4.5%, p = 0.325 |

* Indicates a successful encoding at p < 0.05, Bonferroni corrected for the eight ROIs from the brain atlas by Craddock et al. (2012).

anatomical and functional bases, and to parcellate the surrounding portion of left lateral parietal cortex using the brain atlas by Craddock et al. (2012), resulted in eight ROIs that comprised a wide extension of cortex from the posterior and middle part of intraparietal sulcus (IPS) to superior temporal lobule, angular and supramarginal gyri, as well as superior temporal gyrus, as depicted in Fig. 1, and detailed in Table 1.

The *within-category* RSs obtained from the four models were compared to each other to assess models' collinearity (p < 0.05, Bonferroni corrected). Results were reported in Table 2.

The blind and the sighted *within-category* high-level semantic models were highly correlated (r = 0.68, p < 0.05, Bonferroni corrected). This is consistent with the high correlation value of the whole semantic RS between blind and sighted participants (r = 0.94) previously reported (Handjaras et al., 2016). The other models retained relative lower, not significant correlations (p > 0.05, Bonferroni corrected).

The *within-categories* encoding analysis, performed in the left lateral parietal cortex, indicated a significant ability to discriminate individual concrete nouns using the high-level models (semantic and shape-based perceptual) in the posterior part of the IPS (ROI 2) and in the middle portion of the IPS, extending to the superior parietal lobule (ROI 3). Specifically, in ROI 2, we found an accuracy (average accuracy across presentation modalities ± standard error) of 63.8 ± 1.9% for the semantic high-level model, 59.0 ± 5.2% for the shape-based perceptual model (both p < 0.05, Bonferroni corrected), while the low-level models resulted in a not significant accuracy: 54.8 ± 5.1% for the semantic model based on the perceptual features only and 42.1 ± 3.9% for the GIST-based perceptual one (both p > 0.05).

Similarly, in ROI 3, encoding analysis led to a significant accuracy for the high-level models (60.0 ± 2.9% for the semantic and 60.2 ± 1.6%for the perceptual one, both p < 0.05, Bonferroni corrected) and for the low-level semantic-based model (61.5 ± 1.4%, p < 0.05, Bonferroni corrected), while the low-level perceptual one was at chance level (47.1 ± 3.7%, p > 0.05, Bonferroni corrected). These results were reported in details in Tables 3–6 and Fig. 3.

The two intraparietal ROIs were the only ones that reached significant accuracy across presentation modalities, as the analysis in the other regions of the left parietal cortex, and in the angular gyrus defined both on anatomical or functional constraints, did not reach the significance threshold for any model.

In addition, the same analysis was performed into two primary sensory control regions, bilateral Heschl gyri (HG) and pericalcarine cortex (Cal) and in the left lateral occipital complex (LOC). Overall, the accuracy across presentation modalities in these ROIs did not reach the threshold for significance (p > 0.05, uncorrected for multiple comparisons) apart for the high-level shape-based perceptual model, which achieved a significant discrimination in left LOC (56.0 ± 3.7%, uncorrected p = 0.040).

Here, the similarity encoding procedure aimed at discriminating individual items within each category thus to control for possible biases related to the categorial organization. However, to obtain accuracies comparable to results from previous studies (Anderson et al., 2016b; Mitchell et al., 2008), we performed the encoding analysis exploring the whole RS (i.e., *among-categories* procedure), without restricting to the *within-category* information. Results for the high-level semantic model only were depicted in Fig. 4B and reported in details in the Supplementary Materials. Briefly, the high-level semantic model yielded an overall increase of the accuracy values in the eight ROIs of the left lateral parietal cortex (i.e., +13.5 ± 3.0% on average), when

**Table 4**
***Within-category* individual item encoding accuracies for the high-level perceptual model**. Here are reported the accuracies in each ROI of the encoding procedure in each presentation modality (mean ± standard error) for the perceptual model based on shape features. For Ang AAL, Ang NS, LOC, HG and Cal, please refer to Fig. 1.

| ID ROI | Sighted Pictorial | Sighted Verbal Visual | Sighted Verbal Auditory | Blind Verbal Auditory | Average across modalities |
|---|---|---|---|---|---|
| 1 | 44.2 ± 4.4%, p = 0.771 | 40.0 ± 5.8%, p = 0.903 | 53.3 ± 4.9%, p = 0.307 | 52.5 ± 4.5%, p = 0.327 | 47.5 ± 3.2%, p = 0.743 |
| 2 | 61.7 ± 4.6%, p = 0.037 | 44.2 ± 3.5%, p = 0.754 | 68.3 ± 4.7%, p = 0.006* | 61.7 ± 3.9%, p = 0.052 | 59.0 ± 5.2%, p < 0.001* |
| 3 | 58.3 ± 5.3%, p = 0.110 | 58.3 ± 4.5%, p = 0.111 | 65.0 ± 4.1%, p = 0.015 | 59.2 ± 4.3%, p = 0.095 | 60.2 ± 1.6%, p = 0.003* |
| 4 | 54.2 ± 4.1%, p = 0.274 | 55.8 ± 4.5%, p = 0.185 | 55.0 ± 4.3%, p = 0.256 | 48.3 ± 3.6%, p = 0.572 | 53.3 ± 1.7%, p = 0.203 |
| 5 | 53.3 ± 4.3%, p = 0.288 | 40.0 ± 4.5%, p = 0.892 | 55.8 ± 3.8%, p = 0.185 | 56.7 ± 4.1%, p = 0.154 | 51.5 ± 3.9%, p = 0.328 |
| 6 | 47.5 ± 4.6%, p = 0.617 | 50.0 ± 4.9%, p = 0.474 | 53.3 ± 4.9%, p = 0.317 | 46.7 ± 3.2%, p = 0.634 | 49.4 ± 1.5%, p = 0.548 |
| 7 | 62.5 ± 3.7%, p = 0.036 | 38.3 ± 4.3%, p = 0.945 | 57.5 ± 4.1%, p = 0.148 | 40.8 ± 5.0%, p = 0.878 | 49.8 ± 6.0%, p = 0.499 |
| 8 | 54.2 ± 3.8%, p = 0.269 | 57.5 ± 4.1%, p = 0.139 | 56.7 ± 4.7%, p = 0.158 | 51.7 ± 4.1%, p = 0.381 | 55.0 ± 1.3%, p = 0.095 |
| Ang AAL | 52.5 ± 4.4%, p = 0.344 | 45.0 ± 4.7%, p = 0.701 | 58.3 ± 4.1%, p = 0.121 | 50.0 ± 4.5%, p = 0.457 | 51.5 ± 2.8%, p = 0.345 |
| Ang NS | 49.2 ± 5.0%, p = 0.535 | 55.0 ± 4.0%, p = 0.215 | 60.8 ± 4.6%, p = 0.068 | 47.5 ± 4.3%, p = 0.617 | 53.1 ± 3.0%, p = 0.202 |
| HG | 35.8 ± 4.8%, p = 0.972 | 50.0 ± 4.3%, p = 0.479 | 62.5 ± 4.1%, p = 0.036 | 50.0 ± 4.6%, p = 0.446 | 49.6 ± 5.4%, p = 0.542 |
| Cal | 61.7 ± 4.2%, p = 0.041 | 48.3 ± 4.7%, p = 0.558 | 45.8 ± 5.3%, p = 0.699 | 56.7 ± 4.4%, p = 0.152 | 53.1 ± 3.7%, p = 0.207 |
| LOC | 58.3 ± 3.6%, p = 0.109 | 53.3 ± 4.5%, p = 0.287 | 47.5 ± 3.8%, p = 0.609 | 65.0 ± 3.5%, p = 0.016 | 56.0 ± 3.7%, p = 0.040 |

* Indicates a successful encoding at p < 0.05, Bonferroni corrected for the eight ROIs from the brain atlas by Craddock et al. (2012).

**Table 5**
***Within-category* individual item encoding accuracies for the low-level semantic model**. Here are reported the accuracies in each ROI of the encoding procedure in each presentation modality (mean ± standard error) for the semantic model based on perceptual features only. For Ang AAL, Ang NS, LOC, HG and Cal, please refer to Fig. 1.

| ID ROI | Sighted Pictorial | Sighted Verbal Visual | Sighted Verbal Auditory | Blind Verbal Auditory | Average across modalities |
|---|---|---|---|---|---|
| 1 | 56.7 ± 4.1%, p = 0.163 | 44.2 ± 4.8%, p = 0.765 | 54.2 ± 4.1%, p = 0.287 | 48.3 ± 4.5%, p = 0.558 | 50.8 ± 2.8%, p = 0.413 |
| 2 | 58.3 ± 4.7%, p = 0.108 | 45.8 ± 4.9%, p = 0.697 | 67.5 ± 4.6%, p = 0.005* | 47.5 ± 3.8%, p = 0.631 | 54.8 ± 5.1%, p = 0.090 |
| 3 | 63.3 ± 4.6%, p = 0.029 | 64.2 ± 5.4%, p = 0.014 | 60.0 ± 4.3%, p = 0.077 | 58.3 ± 3.6%, p = 0.133 | 61.5 ± 1.4%, p = 0.004* |
| 4 | 57.5 ± 4.6%, p = 0.154 | 53.3 ± 4.3%, p = 0.291 | 60.0 ± 4.6%, p = 0.079 | 48.3 ± 4.0%, p = 0.565 | 54.8 ± 2.6%, p = 0.091 |
| 5 | 56.7 ± 4.1%, p = 0.161 | 50.8 ± 5.1%, p = 0.411 | 42.5 ± 4.3%, p = 0.851 | 41.7 ± 4.5%, p = 0.869 | 47.9 ± 3.6%, p = 0.742 |
| 6 | 54.2 ± 4.2%, p = 0.271 | 40.8 ± 4.3%, p = 0.874 | 45.8 ± 4.5%, p = 0.685 | 41.7 ± 4.5%, p = 0.851 | 45.6 ± 3.1%, p = 0.895 |
| 7 | 52.5 ± 4.2%, p = 0.360 | 46.7 ± 4.4%, p = 0.652 | 45.8 ± 5.2%, p = 0.694 | 50.0 ± 4.6%, p = 0.470 | 48.8 ± 1.5%, p = 0.650 |
| 8 | 54.2 ± 4.1%, p = 0.253 | 68.3 ± 4.4%, p = 0.005* | 53.3 ± 4.8%, p = 0.306 | 52.5 ± 4.9%, p = 0.334 | 57.1 ± 3.8%, p = 0.034 |
| Ang AAL | 64.2 ± 4.2%, p = 0.025 | 46.7 ± 5.2%, p = 0.651 | 55.8 ± 3.9%, p = 0.180 | 48.3 ± 4.1%, p = 0.575 | 53.8 ± 4.0%, p = 0.130 |
| Ang NS | 58.3 ± 4.3%, p = 0.114 | 45.8 ± 4.6%, p = 0.706 | 57.5 ± 4.7%, p = 0.139 | 44.2 ± 3.3%, p = 0.769 | 51.5 ± 3.7%, p = 0.335 |
| HG | 52.5 ± 4.5%, p = 0.319 | 44.2 ± 4.6%, p = 0.775 | 60.0 ± 4.1%, p = 0.069 | 45.8 ± 4.3%, p = 0.682 | 50.6 ± 3.6%, p = 0.410 |
| Cal | 56.7 ± 4.2%, p = 0.150 | 40.8 ± 4.6%, p = 0.895 | 60.0 ± 4.4%, p = 0.081 | 65.8 ± 3.8%, p = 0.021 | 55.8 ± 5.3%, p = 0.063 |
| LOC | 67.5 ± 3.4%, p = 0.008 | 62.5 ± 4.2%, p = 0.041 | 32.5 ± 3.9%, p = 0.994 | 50.0 ± 4.4%, p = 0.496 | 53.1 ± 7.8%, p = 0.203 |

* Indicates a successful encoding at $p < 0.05$, Bonferroni corrected for the eight ROIs from the brain atlas by Craddock et al. (2012).

using models which were affected by categorial organization. Moreover, all the ROIs in the left parietal cortex resulted to be significant using the *among-categories* procedure ($p < 0.05$, Bonferroni corrected).

## 4. Discussion

To pursue a more comprehensive description of conceptual knowledge organization, this study investigated the specific representation of individual semantic concepts in the angular gyrus and in the neighboring cortical regions within the left lateral parietal cortex, as the extant literature strongly links this area to semantic processing. Patterns of brain activity related to thirty concrete nouns belonging to different categories were analyzed through similarity encoding. Our *within-category* procedure focused on the differences between items belonging to the same category, representing therefore a reliable description of single-item processing, rather than reflecting the superordinate information. In addition, we used four models – two based on linguistic features extracted by a property generation task, and two based on visual computational models applied to pictorial stimuli – to identify brain regions that encode semantic or perceptual properties of single items and to assess whether these representations were more tied to low-level or high-level features.

### 4.1. Similarities and differences of the encoding models

The significant correlation between the high-level semantic models in sighted and congenitally blind individuals, as obtained using the *within-category* approach, confirms the similarity between their representations. Akin results have been previously obtained from the correlation of the whole semantic RS, without controlling for the role of category membership (Handjaras et al., 2016). Therefore, the current finding suggests that the similar high-level semantic representations between the two groups do not merely originate from a common categorial ground (Connolly et al., 2007). Conversely, no significant correlation was achieved when comparing all the semantic models (i.e., low- or high-level) with all other perceptual models, suggesting that the language- and sensory-based descriptions adopted in this study covered different features of the thirty concrete nouns. Of note, the low-level semantic model, albeit based on the subsample of features covering specific sensory information (e.g., shape or color) did not correlate significantly with the high-level semantic model, showing that the selection of features yielded an alternative description of the concrete nouns. Similarly, this low-level semantic model did not correlate between sighted and blind individuals, indicating that it retains specific linguistic features shaped by sensory (i.e., visual or non visual) information (Lenci et al., 2013).

### 4.2. Parietal regions encode perceptual and semantic representations

When selectively focusing on the left angular gyrus only – either anatomically or functionally defined – neither the high-level, nor the low-level models achieved significant accuracy. On the other hand, in the parcellated map that included also the surrounding parietal areas, the *within-category* procedure yielded a successful encoding of the thirty concrete nouns in the intraparietal regions for the high-level models, both semantic and shape-based.

The left lateral parietal region is a key part of the frontoparietal network and is typically associated with attentional tasks focusing on

**Table 6**
***Within-category* individual item encoding accuracies for the low-level perceptual model**. Here are reported the accuracies in each ROI of the encoding procedure in each presentation modality (mean ± standard error) for the perceptual model based on GIST. For Ang AAL, Ang NS, LOC, HG and Cal, please refer to Fig. 1.

| ID ROI | Sighted Pictorial | Sighted Verbal Visual | Sighted Verbal Auditory | Blind Verbal Auditory | Average across modalities |
|---|---|---|---|---|---|
| 1 | 55.8 ± 4.7%, p = 0.186 | 59.2 ± 4.4%, p = 0.086 | 44.2 ± 3.8%, p = 0.785 | 41.7 ± 4.4%, p = 0.866 | 50.2 ± 4.3%, p = 0.493 |
| 2 | 30.8 ± 4.2%, p = 0.997 | 48.3 ± 4.5%, p = 0.569 | 42.5 ± 4.0%, p = 0.836 | 46.7 ± 5.3%, p = 0.646 | 42.1 ± 3.9%, p = 0.993 |
| 3 | 46.7 ± 4.1%, p = 0.669 | 57.5 ± 3.8%, p = 0.124 | 40.8 ± 4.3%, p = 0.874 | 43.3 ± 4.2%, p = 0.812 | 47.1 ± 3.7%, p = 0.817 |
| 4 | 44.2 ± 4.2%, p = 0.770 | 50.0 ± 4.0%, p = 0.511 | 36.7 ± 3.5%, p = 0.958 | 53.3 ± 3.8%, p = 0.284 | 46.0 ± 3.7%, p = 0.888 |
| 5 | 47.5 ± 5.5%, p = 0.606 | 49.2 ± 3.8%, p = 0.522 | 47.5 ± 4.5%, p = 0.601 | 40.8 ± 4.5%, p = 0.894 | 46.2 ± 1.8%, p = 0.848 |
| 6 | 52.5 ± 4.4%, p = 0.366 | 58.3 ± 4.6%, p = 0.117 | 52.5 ± 3.9%, p = 0.343 | 55.8 ± 5.0%, p = 0.204 | 54.8 ± 1.4%, p = 0.100 |
| 7 | 45.8 ± 4.3%, p = 0.695 | 50.8 ± 4.1%, p = 0.419 | 33.3 ± 3.8%, p = 0.988 | 50.8 ± 3.9%, p = 0.438 | 45.2 ± 4.1%, p = 0.911 |
| 8 | 54.2 ± 5.1%, p = 0.287 | 46.7 ± 5.5%, p = 0.672 | 45.8 ± 4.5%, p = 0.688 | 60.0 ± 4.7%, p = 0.077 | 51.7 ± 3.4%, p = 0.349 |
| Ang AAL | 60.8 ± 3.8%, p = 0.067 | 50.0 ± 4.0%, p = 0.503 | 43.3 ± 3.8%, p = 0.793 | 48.3 ± 4.8%, p = 0.567 | 50.6 ± 3.7%, p = 0.432 |
| Ang NS | 52.5 ± 3.4%, p = 0.344 | 60.8 ± 3.5%, p = 0.059 | 43.3 ± 3.7%, p = 0.817 | 55.8 ± 4.3%, p = 0.200 | 53.1 ± 3.7%, p = 0.211 |
| HG | 53.3 ± 5.1%, p = 0.312 | 50.0 ± 5.2%, p = 0.488 | 43.3 ± 4.2%, p = 0.817 | 50.8 ± 4.4%, p = 0.407 | 49.4 ± 2.1%, p = 0.578 |
| Cal | 59.2 ± 4.4%, p = 0.089 | 42.5 ± 5.2%, p = 0.82 | 49.2 ± 4.4%, p = 0.521 | 45.8 ± 3.6%, p = 0.702 | 49.2 ± 3.6%, p = 0.600 |
| LOC | 54.2 ± 4.5%, p = 0.265 | 45.0 ± 4.3%, p = 0.744 | 45.0 ± 4.5%, p = 0.764 | 66.7 ± 4.4%, p = 0.010 | 52.7 ± 5.1%, p = 0.252 |

*Indicates a successful encoding at $p < 0.05$, Bonferroni corrected for the eight ROIs from the brain atlas by Craddock et al. (2012).

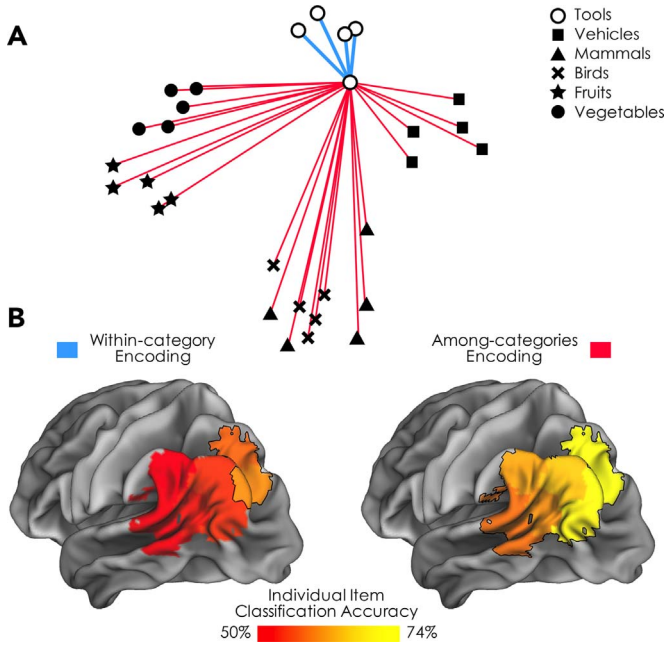


**Fig. 4. Comparison between the *within-category* and *among-categories* procedures.** Panel A: a multidimensional scaling of the high-level semantic RS in sighted subjects. Within- and among- distances for a single item were represented with blue and red lines respectively. Overall, the mean of the within-distances represents about the 55% of the mean of the distances between all the possible pairs of semantic items belonging to different categories in the RS. Panel B left: overall accuracies for the *within-category* procedure. Panel B right: the overall accuracies for the *among-categories* procedure in the left lateral parietal cortex. The *among-categories* procedure yielded an overall increase of the accuracy values of +13.5 ± 3.0% in the left parietal cortex, and all the eight ROIs from the Craddock's atlas resulted to be significant ($p < 0.05$, Bonferroni corrected). The borders of the regions that reported an above-chance accuracy are marked with a solid line (see Supplementary materials for further details).

specific features of a stimulus, i.e. *feature-based attention* (Liu et al., 2011, 2003), or on specific objects in complex environments, i.e. *object-based attention* (Corbetta and Shulman, 2002). However, other studies have reported processing of object features in posterior parietal regions of the dorsal visual pathway to guide actions or motor behavior, and even suggested a strong similarity of object representation between posterior IPS and LOC (Konen and Kastner, 2008; Mruczek et al., 2013). In our study, we report above-chance accuracy for the shape-based model in ROI 2 and 3, which comprises posterior and middle IPS and extends to superior parietal cortex. Of note, we consider the shape-based model as a high-level perceptual description of the items, since it relies on shock-graphs that are robust to object rotation and scaling (Van Eede et al., 2006). Therefore, our finding is in line with a very recent study showing that posterior IPS is not critical for perceptual judgments on object size or orientation (Chouinard et al., 2017),

The low-level perceptual model did not reach above-chance accuracy thresholds neither in the lateral parietal cortex, nor in the primary sensory (though achieving 59.2 ± 4.4%; $p = 0.089$ in Cal for the pictorial modality in sighted individuals) and lateral occipital areas chosen as control regions. This finding suggests that parietal regions do not encode low-level information and that our GIST-based perceptual model allows to control for low-level visual features. Of note, this is in accordance with a previous report, which shows that IPS is recruited for object processing irrespective of spatial frequency modulation (Mahon et al., 2013).

When considering semantic representations, we achieved above-chance accuracies in ROI 2 and ROI 3 for the high-level model, while the low-level one was significant in ROI 3 only. Our findings are consistent with the evidence that left posterior parietal areas are usually activated during experimental tasks involving retrieval and combination of concepts (Seghier and Price, 2012), and single-word processing during sentence reading can even predict response patterns in this area (Anderson et al., 2016a). Hence, both the functional role of the left lateral parietal cortex in semantic processing and autobiographical memory (Seghier and Price, 2012) and its anatomical location and connections (Binder et al., 2009; Friederici, 2009; Price, 2012) strengthen the hypothesis that the angular gyrus and its surrounding regions may represent a key hub to access high-level content of sensory information. This area is also the putative human homologue of the lateral inferior parietal area of the monkey that processes individual items to match them with the superordinate categories they belong to (Freedman and Assad, 2006). Overall, these studies suggest a coding of high-level features in the left intraparietal area, accounting for its role in memory retrieval, combination of concepts and other language-related functions (Price, 2012).

In this study, left LOC showed above-chance accuracy for the high-level perceptual model only. This finding is therefore consistent with the literature suggesting the encoding of object features in this area (Malach et al., 1995; Downing et al., 2007; Konen and Kastner, 2008; Peelen et al., 2014; Papale et al., 2017). In addition, the below-chance accuracy of the high-level semantic model suggests that the role of this region could be more related to the processing of shape-based information. The results in LOC for the shape-based model are mainly driven by blind individuals and are in line with previous studies that identified LOC ability to process object features across different modalities (Peelen et al., 2014; Handjaras et al., 2016; Amedi et al., 2007).

### 4.3. Category-related properties strongly impact on single-item semantic encoding

To account for the impact of the categorial organization of semantic information on single-item discrimination, the analysis was also performed with an *among-categories* approach, thus comparing the activity patterns between all the possible pairs of concrete nouns. The results, reported in Supplementary Materials, show an increased accuracy in the angular gyrus (defined either anatomically or functionally) and in all the regions of the parcellated map. As consequence, all the ROIs in the left parietal cortex reached the significance threshold using the *among-categories* procedure. To further describe the impact of superordinate information within the high-level semantic model, we measured the ratio of the distances between items from the same category and the distances between all the possible pairs of semantic items belonging to different categories, as depicted for illustrative purposes in Fig. 4A. The resulting value of about 0.55 suggests that superordinate categories play a sizable role: this contribute points out that the individual-item semantic encoding may be driven by the differences among superordinate categories, as the increased accuracy values in all ROIs for the *among-categories* encoding confirm (Fig. 4B). This occurrence may arise from broader differences between stimuli, which can be related to the role of superordinate categories per se or by coarse-level distinctions (e.g., living vs. not-living). The relationship between individual semantic items and brain activity patterns during semantic processing have been recently questioned (Barsalou, 2017). In this account, the development of semantic tiles (i.e., the clusters of voxels homogeneously encoding groups of words, as described by Huth et al., 2016) may be shaped by concurrent coarse-level properties which emerge as principal components of the items and subsequently guide their clustering (Huth et al., 2016; Barsalou, 2017). In other words, superordinate categories emerge from major differences between stimuli and can be therefore collinear with global properties of the stimuli (e.g., animacy, concreteness, function). Recently, some authors attempted to encode global properties in brain areas associated with semantic processes, reporting above-chance discrimination for biological categories (Connolly et al., 2012) and natural behaviors (Nastase et al., 2016) in wide cortical patches encompassing multiple brain areas. On the contrary, some individual and well-defined properties of

objects (i.e., manipulability: Mahon et al., 2013) or animals (i.e., dangerousness: Connolly et al., 2016) were specifically decoded from brain activity in IPS. In light of this, the large extent of parietal cortex achieved in our study by the *among-categories* encoding of individual items should be interpreted as a lack in specificity, due to the major role played here by superordinate information and its associated global properties. Whether these global properties, widely distributed on the human cortex, retain an essential role in conceptual representations of individual items is still matter of debate (Barsalou et al., 2017). We speculate that areas like the angular gyrus may process superordinate features only, therefore representing concepts at a higher level of abstraction through a hierarchical conjunctive coding (Barsalou, 2016; Binder, 2016). These results highlight the need to control for category-driven differences – as we did in our *within-category* individual item encoding – as this represents the best possible way to disentangle the role of coarse and fine differences between concepts in semantic studies.

### 4.4. The role of the property-generation task. Methodological considerations and limitations

The results from the high- and low-level models in the IPS suggest that this region is not simply recruited by sensory-specific information in a bottom-up manner (Ibos and Freedman, 2016), but, conversely, encodes higher-level feature-based representations. This is consistent with previous reports (Scolari et al., 2015) and with the overlapping activation of intraparietal cortex during semantic processing, previously observed in sighted and congenitally blind individuals during single word processing (Noppeney et al., 2003). Since results were above chance in both sighted and congenitally blind individuals, we posit that the left IPS encodes representations, independent from sensory modality and not related to visual imagery (Ricciardi et al., 2014a, 2014b; Ricciardi and Pietrini, 2011).

Of note, lateral and posterior parietal areas have been traditionally associated with feature binding tasks, during which object features processed in separate maps are spatially and temporally integrated to produce a unified perceptual and cognitive experience (Robertson, 2003; Scolari et al., 2015; Shafritz et al., 2002; Treisman and Gelade, 1980). Additional evidence of the binding role of parietal areas were provided by neuropsychological studies that showed patients with lesions in posterior parietal regions which fail to conjoin different visual features related to the same object (Friedman-Hill et al., 1995; Robertson et al., 1997; Treisman and Gelade, 1980). Even if we may suppose the binding of perceptual and semantic features to be fundamental for a finer-grained description of individual items, we cannot exclude that the *within-category* encoding in latero-posterior parietal cortex could be more related to the property generation task, rather than to conceptual processing. Indeed, the property generation task, similar to a feature binding task, relied on the association of properties to concrete nouns. We assume that the nature of the task, combined with an analysis aimed at evidencing the differences between the representations of single nouns, could account for the recruitment of the intraparietal cortex (Bonnici et al., 2016; Handjaras et al., 2016; Pulvermuller, 2013). The extent of the association between the activity in posterior parietal regions and the task used should be investigated by future studies, in which single-item semantic processing is analyzed through different tasks which do not require an active manipulation of the words.

Some additional limitations of our study also should be highlighted. First, the analysis was conducted on a single group-level neural RS, obtained from the average of the five individual RSs for each presentation modality. While this can be considered as an estimation of a group-level representation (Carlson et al., 2014; Kriegeskorte et al., 2008), this RS does not consider differences between individual subjects (i.e., each subject's own conceptual representation), that may play a greater role in single-item semantic studies as compared to studies employing category-based models (Charest et al., 2014). Moreover, group-level RSs, although commonly used to increase signal-to-noise ratio of fMRI activity patterns (Carlson et al., 2014; Kriegeskorte et al., 2008) – a mandatory requirement to perform single item encoding – do not take into account the random-effect model. This limitation affects the generalizability of these findings. In addition, the *within-category* encoding was performed only on a small number of examples, as each category contained only five different items. Further studies may benefit greatly from more accurate models that compare a greater number of concrete nouns while controlling for their category membership. Finally, the analyses were performed on a single parcellation of the left parietal cortex, chosen *a priori* on the basis of an atlas based on resting-state functional activity (Craddock et al., 2012). For this reason, we can not exclude that different parcellation criteria (e.g., the choice of a different atlas or a different number of ROIs) can yield different results in the encoding analysis, mainly due to the dependence of the accuracy on the size and signal-to-noise ratio of the chosen ROIs. Another potential limitation regards the choice of averaging the encoding performances across different groups. Our previous study using the same data has reported that the semantic information in the left lateral parietal cortex is consistent across all presentation modalities (Handjaras et al., 2016). In addition, a recent study has reported highly similar activity patterns for pictorial and word-based representation of natural scenes in posterior IPS, showing that brain patterns elicited by pictures can be decoded by a classifier trained on words, and vice-versa (Kumar et al., 2017). This confirms that the presentation modality does not play an important role in driving semantic processing in this region.

In conclusion, this study shows that the processing of high-level features – both semantic and perceptual (i.e., shapes) engages to different degrees individual sub-regions of the left lateral parietal cortex, showing higher accuracy in the intraparietal sulcus, whose activity was predicted using a high-level models that accounted for the differences between individual concepts. Conversely, high accuracy in a large extent of parietal cortex comprising the angular gyrus and its neighboring regions can be achieved only when the information regarding superordinate categories is retained. Overall, these results indicate the need to control for the coarse-level categorial organization when performing studies on higher-level processes related to the retrieval of semantic information, such as language and autobiographical memory.

## Author contributions

E.R., P.P., A. Lenci and G.M. conceived the study; G.H., A. Leo, L.C., A. Lenci and E.R. designed the experiment; A. Leo, L.C. acquired the data; G.H., A. Leo, P. Papale and L.C. analyzed the data; all authors interpreted the results; G.H., A. Leo, L.C., P. Papale and E.R. drafted the manuscript; P.P., A. Lenci and G.M. critically revised the manuscript.

## Conflicts of interest

None declared.

## Funding

This work was supported by Italian Grants “Semantic representations in the language of the blind: linguistic and neurocognitive studies” (PRIN 2008CM9MY3), “A multimodal approach to the structural and functional characterization of supramodality in the blind brain” (PRIN 2015AR52F9), “Aesthetics in the Brain: an interdisciplinary investigation on the functional and neural mechanisms mediating aesthetic experience” (PRIN 2015WXAXJF) and by Fondazione Cassa di Risparmio di Lucca (Lucca, Italy).

## Acknowledgments

We thank the Unione Italiana Ciechi (National Association for the Blind) for their collaboration, and the anonymous reviewers for their constructive comments.

## Appendix A. Supplementary material

Supplementary data associated with this article can be found in the online version at http://dx.doi.org/10.1016/j.neuropsychologia.2017.05.001.

## References

Amedi, A., Stern, W.M., Camprodon, J.A., Bermpohl, F., Merabet, L., Rotman, S., Hemond, C., Meijer, P., Pascual-Leone, A., 2007. Shape conveyed by visual-to-auditory sensory substitution activates the lateral occipital complex. Nat. Neurosci. 10, 687–689.

Anderson, A.J., Binder, J.R., Fernandino, L., Humphries, C.J., Conant, L.L., Aguilar, M., Wang, X., Doko, D., Raizada, R.D., 2016a. Predicting neural activity patterns associated with sentences using a neurobiologically motivated model of semantic representation. Cereb. Cortex.

Anderson, A.J., Zinszer, B.D., Raizada, R.D., 2016b. Representational similarity encoding for fMRI: pattern-based synthesis to predict brain activity using stimulus-model-similarities. Neuroimage 128, 44–53.

Andersson, J.L., Jenkinson, M., Smith, S., 2007. Non-linear optimisation. FMRIB technical report TR07JA1. Practice. 2007a Jun.

Baldassi, C., Alemi-Neissi, A., Pagan, M., Dicarlo, J.J., Zecchina, R., Zoccolan, D., 2013. Shape similarity, better than semantic membership, accounts for the structure of visual object representations in a population of monkey inferotemporal neurons. PLoS Comput. Biol. 9, e1003167.

Barsalou, L.W., 2016. On staying grounded and avoiding quixotic dead ends. Psychon. Bull. Rev. 23, 1122–1142.

Barsalou, L.W., 2017. What does semantic tiling of the cortex tell us about semantics? Neuropsychologia.

Bi, Y., Wang, X., Caramazza, A., 2016. Object domain and modality in the ventral visual pathway. Trends Cogn. Sci. 20, 282–290.

Binder, J.R., 2016. In defense of abstract conceptual representations. Psychon. Bull. Rev. 23, 1096–1108.

Binder, J.R., Desai, R.H., Graves, W.W., Conant, L.L., 2009. Where is the semantic system? A critical review and meta-analysis of 120 functional neuroimaging studies. Cereb. Cortex 19, 2767–2796.

Blum, H., 1973. Biological shape and visual science (Part I). J. Theor. Biol. 38, 205–287.

Bona, S., Cattaneo, Z., Silvanto, J., 2015. The causal role of the occipital face area (OFA) and lateral occipital (LO) cortex in symmetry perception. J. Neurosci. 35, 731–738.

Bonnici, H.M., Richter, F.R., Yazar, Y., Simons, J.S., 2016. Multimodal feature integration in the angular gyrus during episodic and semantic retrieval. J. Neurosci. 36, 5462–5471.

Bracci, S., Op de Beeck, H., 2016. Dissociations and associations between shape and category representations in the two visual pathways. J. Neurosci. 36, 432–444.

Carlson, T.A., Simmons, R.A., Kriegeskorte, N., Slevc, L.R., 2014. The emergence of semantic meaning in the ventral temporal pathway. J. Cogn. Neurosci. 26, 120–131.

Charest, I., Kievit, R.A., Schmitz, T.W., Deca, D., Kriegeskorte, N., 2014. Unique semantic space in the brain of each beholder predicts perceived similarity. Proc. Natl. Acad. Sci. USA 111, 14565–14570.

Chouinard, P.A., Meena, D.K., Whitwell, R.L., Hilchey, M.D., Goodale, M.A., 2017. A TMS investigation on the role of lateral occipital and caudal intraparietal sulcus in the perception of object form and orientation. J. Cogn. Neurosci.

Clarke, A., Tyler, L.K., 2015. Understanding what we see: how we derive meaning from vision. Trends Cogn. Sci. 19, 677–687.

Connolly, A.C., Gleitman, L.R., Thompson-Schill, S.L., 2007. Effect of congenital blindness on the semantic representation of some everyday concepts. Proc. Natl. Acad. Sci. USA 104, 8241–8246.

Connolly, A.C., Guntupalli, J.S., Gors, J., Hanke, M., Halchenko, Y.O., Wu, Y.-C., Abdi, H., Haxby, J.V., 2012. The representation of biological classes in the human brain. J. Neurosci. 32, 2608–2618.

Connolly, A.C., Sha, L., Guntupalli, J.S., Oosterhof, N., Halchenko, Y.O., Nastase, S.A., di Oleggio Castello, M.V., Abdi, H., Jobst, B.C., Gobbini, M.I., 2016. How the human brain represents perceived dangerousness or "predacity" of animals. J. Neurosci. 36, 5373–5384.

Corbetta, M., Shulman, G.L., 2002. Control of goal-directed and stimulus-driven attention in the brain. Nat. Rev. Neurosci. 3, 201–215.

Cox, R.W., 1996. AFNI: software for analysis and visualization of functional magnetic resonance neuroimages. Comput. Biomed. Res 29, 162–173.

Craddock, R.C., James, G.A., Holtzheimer 3rd, P.E., Hu, X.P., Mayberg, H.S., 2012. A whole brain fMRI atlas generated via spatially constrained spectral clustering. Hum. Brain Mapp. 33, 1914–1928.

Downing, P.E., Wiggett, A.J., Peelen, M.V., 2007. Functional magnetic resonance imaging investigation of overlapping lateral occipitotemporal activations using multi-voxel pattern analysis. J. Neurosci. 27, 226–233.

Efron, B., Tibshirani, R.J., 1994. An Introduction to the Bootstrap. CRC press.

Eickhoff, S.B., Paus, T., Caspers, S., Grosbras, M.H., Evans, A.C., Zilles, K., Amunts, K., 2007. Assignment of functional activations to probabilistic cytoarchitectonic areas revisited. Neuroimage 36, 511–521.

Fernandino, L., Binder, J.R., Desai, R.H., Pendl, S.L., Humphries, C.J., Gross, W.L., Conant, L.L., Seidenberg, M.S., 2016. Concept representation reflects multimodal abstraction: a framework for embodied semantics. Cereb. Cortex 26, 2018–2034.

Freedman, D.J., Assad, J.A., 2006. Experience-dependent representation of visual categories in parietal cortex. Nature 443, 85–88.

Friederici, A.D., 2009. Pathways to language: fiber tracts in the human brain. Trends Cogn. Sci. 13, 175–181.

Friedman-Hill, S.R., Robertson, L.C., Treisman, A., 1995. Parietal contributions to visual feature binding: evidence from a patient with bilateral lesions. Science 269, 853–855.

Gainotti, G., 2010. The influence of anatomical locus of lesion and of gender-related familiarity factors in category-specific semantic disorders for animals, fruits and vegetables: a review of single-case studies. Cortex 46, 1072–1087.

Ghio, M., Vaghi, M.M., Perani, D., Tettamanti, M., 2016. Decoding the neural representation of fine-grained conceptual categories. Neuroimage 132, 93–103.

Handjaras, G., Bernardi, G., Benuzzi, F., Nichelli, P.F., Pietrini, P., Ricciardi, E., 2015. A topographical organization for action representation in the human brain. Hum. Brain Mapp. 36, 3832–3844.

Handjaras, G., Ricciardi, E., Leo, A., Lenci, A., Cecchetti, L., Cosottini, M., Marotta, G., Pietrini, P., 2016. How concepts are encoded in the human brain: a modality independent, category-based cortical organization of semantic knowledge. Neuroimage 135, 232–242.

Huth, A.G., de Heer, W.A., Griffiths, T.L., Theunissen, F.E., Gallant, J.L., 2016. Natural speech reveals the semantic maps that tile human cerebral cortex. Nature 532, 453–458.

Ibos, G., Freedman, D.J., 2016. Interaction between spatial and feature attention in posterior parietal cortex. Neuron 91, 931–943.

Jackson, R.L., Hoffman, P., Pobric, G., Lambon Ralph, M.A., 2016. The semantic network at work and rest: differential connectivity of anterior temporal lobe subregions. J. Neurosci. 36, 1490–1501.

Jozwik, K.M., Kriegeskorte, N., Mur, M., 2016. Visual features as stepping stones toward semantics: explaining object similarity in IT and perception with non-negative least squares. Neuropsychologia 83, 201–226.

Kaiser, D., Azzalini, D.C., Peelen, M.V., 2016. Shape-independent object category responses revealed by MEG and fMRI decoding. J. Neurophysiol. 115, 2246–2250.

Kemmerer, D., 2016. Categories of object concepts across languages and brains: the relevance of nominal classification systems to cognitive neuroscience. Lang., Cogn. Neurosci. 0, 1–24.

Khaligh-Razavi, S.M., Kriegeskorte, N., 2014. Deep supervised, but not unsupervised, models may explain IT cortical representation. PLoS Comput. Biol. 10, e1003915.

Konen, C.S., Kastner, S., 2008. Two hierarchically organized neural systems for object information in human visual cortex. Nat. Neurosci. 11, 224–231.

Kremer, G., Baroni, M., 2011. A set of semantic norms for German and Italian. Behav. Res Methods 43, 97–109.

Kriegeskorte, N., Mur, M., Ruff, D.A., Kiani, R., Bodurka, J., Esteky, H., Tanaka, K., Bandettini, P.A., 2008. Matching categorical object representations in inferior temporal cortex of man and monkey. Neuron 60, 1126–1141.

Kubilius, J., Wagemans, J., Op de Beeck, H.P., 2014. A conceptual framework of computations in mid-level vision. Front Comput. Neurosci. 8, 158.

Kumar, M., Federmeier, K.D., Fei-Fei, L., Beck, D.M., 2017. Evidence for similar patterns of neural activity elicted by picture-and word-based representations of natural scenes. Neuroimage.

Leeds, D.D., Seibert, D.A., Pyles, J.A., Tarr, M.J., 2013. Comparing visual representations across human fMRI and computational vision. J. Vision. 13 (25-25).

Lenci, A., Baroni, M., Cazzolli, G., Marotta, G., 2013. BLIND: a set of semantic feature norms from the congenitally blind. Behav. Res Methods 45, 1218–1233.

Leo, A., Handjaras, G., Bianchi, M., Marino, H., Gabiccini, M., Guidi, A., Scilingo, E.P., Pietrini, P., Bicchi, A., Santello, M., Ricciardi, E., 2016. A synergy-based hand control is encoded in human motor cortical areas. Elife 5.

Liu, T., Slotnick, S.D., Serences, J.T., Yantis, S., 2003. Cortical mechanisms of feature-based attentional control. Cereb. Cortex 13, 1334–1343.

Liu, T., Hospadaruk, L., Zhu, D.C., Gardner, J.L., 2011. Feature-specific attentional priority signals in human cortex. J. Neurosci. 31, 4484–4495.

Mahon, B.Z., Caramazza, A., 2009. Concepts and categories: a cognitive neuropsychological perspective. Annu Rev. Psychol. 60, 27–51.

Mahon, B.Z., Caramazza, A., 2011. What drives the organization of object knowledge in the brain? Trends Cogn. Sci. 15, 97–103.

Mahon, B.Z., Kumar, N., Almeida, J., 2013. Spatial frequency tuning reveals interactions between the dorsal and ventral visual systems. J. Cogn. Neurosci. 25, 862–871.

Malach, R., Reppas, J., Benson, R., Kwong, K., Jiang, H., Kennedy, W., Ledden, P., Brady, T., Rosen, B., Tootell, R., 1995. Object-related activity revealed by functional magnetic resonance imaging in human occipital cortex. Proc. Natl. Acad. Sci. 92, 8135–8139.

McRae, K., Cree, G.S., Seidenberg, M.S., McNorgan, C., 2005. Semantic feature production norms for a large set of living and nonliving things. Behav. Res Methods 37, 547–559.

Mitchell, T.M., Shinkareva, S.V., Carlson, A., Chang, K.M., Malave, V.L., Mason, R.A., Just, M.A., 2008. Predicting human brain activity associated with the meanings of nouns. Science 320, 1191–1195.

Mruczek, R.E., von Loga, I.S., Kastner, S., 2013. The representation of tool and non-tool object information in the human intraparietal sulcus. J. Neurophysiol. 109, 2883–2896.

Nastase, S.A., Connolly, A.C., Oosterhof, N.N., Halchenko, Y.O., Guntupalli, J.S., di Oleggio Castello, M.V., Gors, J., Gobbini, M.I., Haxby, J.V., 2016. Attention

selectively reshapes the geometry of distributed semantic representation. bioRxiv 045252.
Nichols, T.E., Holmes, A.P., 2002. Nonparametric permutation tests for functional neuroimaging: a primer with examples. Human. Brain Mapp. 15, 1–25.
Noppeney, U., Friston, K.J., Price, C.J., 2003. Effects of visual deprivation on the organization of the semantic system. Brain 126, 1620–1627.
Oliva, A., Torralba, A., 2001. Modeling the shape of the scene: a holistic representation of the spatial envelope. Int. J. Comput. Vision. 42, 145–175.
Papale, P., Leo, A., Cecchetti, L., Handjaras, G., Kay, K., Pietrini, P., Ricciardi, E., 2017. Foreground enhancement and background suppression in human early visual system During passive perception of natural images. bioRxiv 109496.
Peelen, M.V., He, C., Han, Z., Caramazza, A., Bi, Y., 2014. Nonvisual and visual object shape representations in occipitotemporal cortex: evidence from congenitally blind and sighted adults. J. Neurosci. 34, 163–170.
Price, A.R., Bonner, M.F., Peelle, J.E., Grossman, M., 2015. Converging evidence for the neuroanatomic basis of combinatorial semantics in the angular gyrus. J. Neurosci. 35, 3276–3284.
Price, C.J., 2012. A review and synthesis of the first 20 years of PET and fMRI studies of heard speech, spoken language and reading. Neuroimage 62, 816–847.
Proklova, D., Kaiser, D., Peelen, M.V., 2016. Disentangling representations of object shape and object category in human visual cortex: the animate-inanimate distinction. J. Cogn. Neurosci. 28, 680–692.
Pulvermuller, F., 2013. How neurons make meaning: brain mechanisms for embodied and abstract-symbolic semantics. Trends Cogn. Sci. 17, 458–470.
Ricciardi, E., Pietrini, P., 2011. New light from the dark: what blindness can teach us about brain function. Curr. Opin. Neurol. 24, 357–363.
Ricciardi, E., Bonino, D., Pellegrini, S., Pietrini, P., 2014a. Mind the blind brain to understand the sighted one! Is there a supramodal cortical functional architecture? Neurosci. Biobehav Rev. 41, 64–77.
Ricciardi, E., Handjaras, G., Pietrini, P., 2014b. The blind brain: how (lack of) vision shapes the morphological and functional architecture of the human brain. Exp. Biol. Med (Maywood) 239, 1414–1420.
Rice, G.E., Watson, D.M., Hartley, T., Andrews, T.J., 2014. Low-level image properties of visual objects predict patterns of neural response across category-selective regions of the ventral visual pathway. J. Neurosci. 34, 8837–8844.
Robertson, L., Treisman, A., Friedman-Hill, S., Grabowecky, M., 1997. The Interaction of Spatial and Object Pathways: evidence from Balint's Syndrome. J. Cogn. Neurosci. 9, 295–317.
Robertson, L.C., 2003. Binding, spatial attention and perceptual awareness. Nat. Rev. Neurosci. 4, 93–102.
Scolari, M., Seidl-Rathkopf, K.N., Kastner, S., 2015. Functions of the human frontoparietal attention network: evidence from neuroimaging. Curr. Opin. Behav. Sci. 1, 32–39.
Sebastian, T.B., Klein, P.N., Kimia, B.B., 2004. Recognition of shapes by editing their shock graphs. IEEE Trans. Pattern Anal. Mach. Intell. 26, 550–571.
Seghier, M.L., 2013. The angular gyrus: multiple functions and multiple subdivisions. Neuroscientist 19, 43–61.
Seghier, M.L., Price, C.J., 2012. Functional heterogeneity within the default network during semantic processing and speech production. Front Psychol. 3, 281.
Shafritz, K.M., Gore, J.C., Marois, R., 2002. The role of the parietal cortex in visual feature binding. Proc. Natl. Acad. Sci. USA 99, 10917–10922.
Smith, S.M., Jenkinson, M., Woolrich, M.W., Beckmann, C.F., Behrens, T.E., Johansen-Berg, H., Bannister, P.R., De Luca, M., Drobnjak, I., Flitney, D.E., Niazy, R.K., Saunders, J., Vickers, J., Zhang, Y., De Stefano, N., Brady, J.M., Matthews, P.M., 2004. Advances in functional and structural MR image analysis and implementation as FSL. Neuroimage 23 (Suppl 1), S208–S219.
Treisman, A.M., Gelade, G., 1980. A feature-integration theory of attention. Cogn. Psychol. 12, 97–136.
Tyler, L.K., Chiu, S., Zhuang, J., Randall, B., Devereux, B.J., Wright, P., Clarke, A., Taylor, K.I., 2013. Objects and categories: feature statistics and object processing in the ventral stream. J. Cogn. Neurosci. 25, 1723–1735.
Tzourio-Mazoyer, N., Landeau, B., Papathanassiou, D., Crivello, F., Etard, O., Delcroix, N., Mazoyer, B., Joliot, M., 2002. Automated anatomical labeling of activations in SPM using a macroscopic anatomical parcellation of the MNI MRI single-subject brain. Neuroimage 15, 273–289.
Van Eede, M., Macrini, D., Telea, A., Sminchisescu, C., Dickinson, S., 2006. Canonical skeletons for shape matching. Pattern Recognition, 2006. ICPR 2006. In: Proceedings of the 18th International Conference on. IEEE, pp. 64–69.
Vigliocco, G., Kousta, S.T., Della Rosa, P.A., Vinson, D.P., Tettamanti, M., Devlin, J.T., Cappa, S.F., 2014. The neural representation of abstract words: the role of emotion. Cereb. Cortex 24, 1767–1777.
Wang, X., Peelen, M.V., Han, Z., He, C., Caramazza, A., Bi, Y., 2015. How visual is the visual cortex? comparing connectional and functional fingerprints between congenitally blind and sighted individuals. J. Neurosci. 35, 12545–12559.
Wang, X., Peelen, M.V., Han, Z., Caramazza, A., Bi, Y., 2016. The role of vision in the neural representation of unique entities. Neuropsychologia 87, 144–156.
Watson, D.M., Young, A.W., Andrews, T.J., 2016. Spatial properties of objects predict patterns of neural response in the ventral visual pathway. Neuroimage 126, 173–183.
Wu, L.L., Barsalou, L.W., 2009. Perceptual simulation in conceptual combination: evidence from property generation. Acta Psychol. 132, 173–189.
Yarkoni, T., Poldrack, R.A., Nichols, T.E., Van Essen, D.C., Wager, T.D., 2011. Large-scale automated synthesis of human functional neuroimaging data. Nat. Methods 8, 665–670.